

Ocean carbon uptake and storage influenced by wind bias in global climate models

N. C. Swart^{1*} and J. C. Fyfe²

In global climate model pre-industrial control simulations the Southern Hemisphere westerly winds show a systematic bias in position and strength relative to estimates of their actual position and strength. These wind-stress biases impact the simulated transport of the Antarctic Circumpolar Current¹ and the nature of Southern Ocean water-mass formation¹ and may affect the rate of meridional overturning of the global ocean². The effect they have on oceanic carbon uptake and storage is unknown, however. Here we demonstrate, using a coupled carbon-climate model³, that the wind-stress biases reduce equilibrium ocean carbon storage, redistribute carbon within the ocean and increase oceanic carbon uptake in climate change simulations. The wind-stress biases act directly by influencing Ekman pumping dynamics in the Southern Ocean and also seem to have an indirect effect on the overturning circulation and carbon distribution through the Agulhas leakage and Indo-Atlantic salt flux. Our results indicate that carbon-climate model simulations with the typical pre-industrial wind-stress bias will over-estimate ocean carbon sequestration, and thereby under-estimate atmospheric carbon dioxide concentrations in the twenty-first century, relative to unbiased simulations. The new generation of coupled carbon-climate models may be subject to these wind biases, which could alter their carbon-climate response, although it is worth noting that the uncertainty arising from wind biases that we demonstrate here is one of several uncertainties that affect modelled ocean carbon uptake⁴.

The uncertainties in ocean carbon uptake include uncertainties in the physical circulation due to poorly resolved dynamics⁵, incorrect wind-stress forcing at the ocean surface^{6,7}, as well as other uncertainties such as the rate of biological carbon sequestration^{4,8}. Our study isolates and quantifies the uncertainty associated with one of these factors, the surface wind stress.

The Southern Hemisphere westerly winds exhibit an equatorward-biased position and anomalous strength in the pre-industrial control experiments of the Coupled Model Intercomparison Project Phase 3 (CMIP3) models⁹, relative to observed pre-industrial winds (see Supplementary Information S1). However, the effect of the wind-stress biases on ocean carbon storage in the CMIP3 models has not been directly evaluated because those models do not include interactive carbon cycles⁷. The new generation of carbon-climate models, a subset of CMIP5, now include carbon cycles, which allows them to track the flow of carbon through the Earth system¹⁰. However, intermodel comparisons are confounded by differences in ocean mixing schemes and other factors¹, which independently influence carbon uptake and may obscure the role of the wind-stress bias.

To isolate the influence of pre-industrial wind-stress biases on ocean carbon we have designed an experiment that eliminates the confounding physical differences between models. We do this by using the University of Victoria Earth System Climate Model³ (UVic ESCM) as the common framework. The UVic ESCM uses a two-dimensional energy balance atmospheric model, and this allows us to specify the ocean-surface wind-stress fields. We produced an ensemble of experiments by forcing the UVic ESCM with the pre-industrial wind-stress climatologies from 18 CMIP3 coupled atmosphere-ocean global climate models. These 18 CMIP3 wind-stress experiments were all started from the same control state, and integrated for 7,000 years each under 1850 atmospheric CO₂ concentrations, to produce pre-industrial equilibria. The CMIP3 experiments are compared with a 7,000-year control simulation that was forced with an observationally derived pre-industrial wind-stress climatology (see Methods).

Total ocean carbon storage adjusted to new equilibria over several thousand years in the CMIP3 wind-stress experiments (Fig. 1a). The ocean holds less carbon in the wind-stress-biased CMIP3 experiments than in the control simulation that used observed pre-industrial winds. The total range in carbon storage amongst the runs after 7,000 years is around 400 Pg, a small fraction of total ocean carbon, but a significant change with respect to the atmospheric carbon reservoir of about 600 Pg. The differences in ocean carbon storage between CMIP3 equilibrium experiments are due to direct wind-stress impacts on the air-sea CO₂ fluxes (Fig. 1b,c; wind-speed effects are excluded here, but do not change our result. See Supplementary Information S2).

The period required to equilibrate ocean carbon under the CMIP3 wind stresses is set by the altered surface CO₂ flux, combined with the overturning timescale required to ventilate the oceanic interior. Changes in the biological pump were relatively minor, and cannot explain the changes in ocean carbon storage. The main adjustment to equilibrium of the ensemble mean over the first 2,000 years (Fig. 1a) was driven by the time-integrated surface CO₂ flux anomaly (Fig. 1c). The flux anomalies were distributed across the surface of the world ocean, but were most prominent in the Southern Ocean. In the zonal integral, the ocean south of 30° S accounted for more than 80% of the variability in global CO₂ surface flux. The decrease in ensemble mean total ocean carbon was principally driven by anomalous outgassing between 40° S and 60° S. Here, the wind-stress bias drove upwelling of carbon-rich deep waters through a positive Ekman pumping anomaly (Fig. 1c), which subsequently outgassed to the atmosphere. A compensatory enhanced in-gassing occurred between 20° S and 40° S owing to anomalous downwelling there, but its integrated effect is significantly smaller. Southern Ocean circulation anomalies

¹School of Earth and Ocean Sciences, University of Victoria, Victoria, British Columbia V8W 3V6, Canada, ²Canadian Centre for Climate Modelling and Analysis, Environment Canada, Victoria, British Columbia V8W 3V6, Canada. *e-mail: ncswart@uvic.ca.

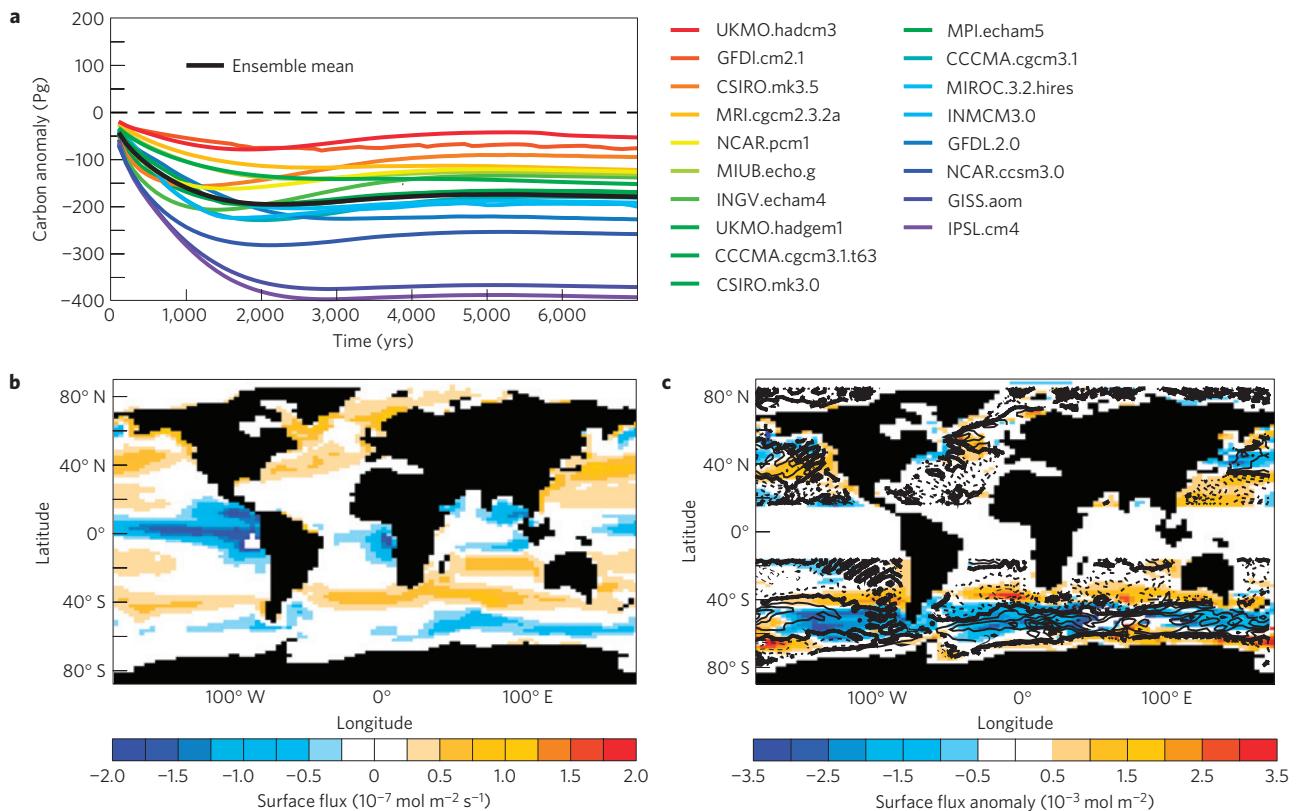


Figure 1 | Evolution of ocean carbon to equilibrium. **a**, Ocean total carbon anomaly for 18 CMIP3 wind-stress experiments (coloured lines) with the ensemble mean shown in black. The anomaly is computed relative to the control simulation. **b**, Ensemble mean surface CO_2 flux of the 18 CMIP3 experiments at 7,000 years. **c**, The shading shows the ensemble mean surface CO_2 flux anomaly, relative to the control, integrated from 0 to 2,000 years. Negative values (blue shades) indicate anomalous outgassing from the ocean. The contours show the ensemble mean Ekman pumping anomaly (positive values, the solid contours, indicate increased upwelling). The area 15°S – 15°N , where the Ekman pumping anomaly is not well defined has been masked. Equilibrium experiments were conducted under 1850 forcing, and only surface wind stress varies between runs.

due to wind-stress biases may be smaller in models with higher spatial resolution than ours, but are likely to remain substantial⁵.

Wind-stress biases also lead to a redistribution of carbon within the ocean. The CMIP3 experiments exhibit an increase in Atlantic carbon storage, and a decrease in Pacific carbon storage, on average, relative to the control (Fig. 2a). The changes amount to only several per cent of the total carbon storage locally, but again represent a significant fraction of the atmospheric reservoir. The inter-basin redistribution of carbon cannot readily be explained by surface CO_2 flux changes, which were nearly zonally symmetric (Fig. 1c). Rather, the Atlantic accumulation of carbon occurred principally between 500 and 4,000 m, north of 40°S and was associated with a slowdown in the meridional overturning circulation (MOC; Fig. 2b).

The MOC slowdown resulted from changes in the Agulhas leakage. The Agulhas leakage refers to the transport of Indian Ocean water into the South Atlantic via the Agulhas retroflection south of Africa, and is the principal conduit for Indo–Atlantic exchange¹¹. Variability in Agulhas leakage strength is linked to Atlantic MOC variability on centennial to millennial timescales by palaeo-observations¹², and Atlantic salinity trends in modern observational records¹³. Previous modelling studies have shown that the Agulhas leakage modulates MOC strength through the Indo–Atlantic exchange of salt¹⁴, and contributes to MOC variability on decadal¹⁵ to millennial timescales^{2,16}.

The strength of the Agulhas leakage depends on the latitude of the zero in wind-stress curl in the Indian Ocean south of Africa^{2,13}. In our equilibrium experiments, models with equatorward positions of the zero wind-stress curl exhibit reduced Agulhas leakage (Fig. 3a) and Indo–Atlantic salt exchange. Models with a reduction

in the Indo–Atlantic salt flux in turn experienced a freshening of the near-surface North Atlantic (Fig. 3b). Here, vertical density gradients are more salinity dependent, and hence North Atlantic convection was reduced proportionally to the degree of freshening associated with a reduced Agulhas leakage (Fig. 3c). A reduction in the deep-water formation rate is what led to a slowdown in the Atlantic MOC (Fig. 3d). A slower MOC, with reduced Indo–Atlantic exchange then caused the accumulation of carbon in the Atlantic and reduction in Pacific carbon storage that we see in the CMIP3 experiments (Fig. 3e). Thus, the relative degree of Atlantic carbon accumulation is directly dependent on the volume flux of the Agulhas leakage (Fig. 3f). Note however that mesoscale eddies, which our model does not explicitly resolve, may also influence Agulhas leakage–MOC dynamics (see Supplementary Information S3).

Differences in equilibrium ocean carbon storage affect the oceanic uptake of carbon during time-evolving (transient) climate-change simulations. Transient simulations spanning the period 1850–2200 were launched from the end of the 7,000-year equilibrium experiments. Atmospheric CO_2 was allowed to evolve freely and carbon emissions were specified following scenario A2 of the *Special Report on Emissions Scenarios*¹⁷ (SRES), for both the CMIP3 experiments and the observed wind-stress control simulation. In the transient experiments, we continued to force the 18-member ensemble with the CMIP3 pre-industrial winds and the control simulation forcing remained the observed pre-industrial wind stress. We held the wind stress fixed, rather than evolving, so that we could isolate the effect of the pre-industrial wind-stress bias on the transient simulations. Varying the wind stress during these simulations (as in ref. 18) would make it impossible to differentiate

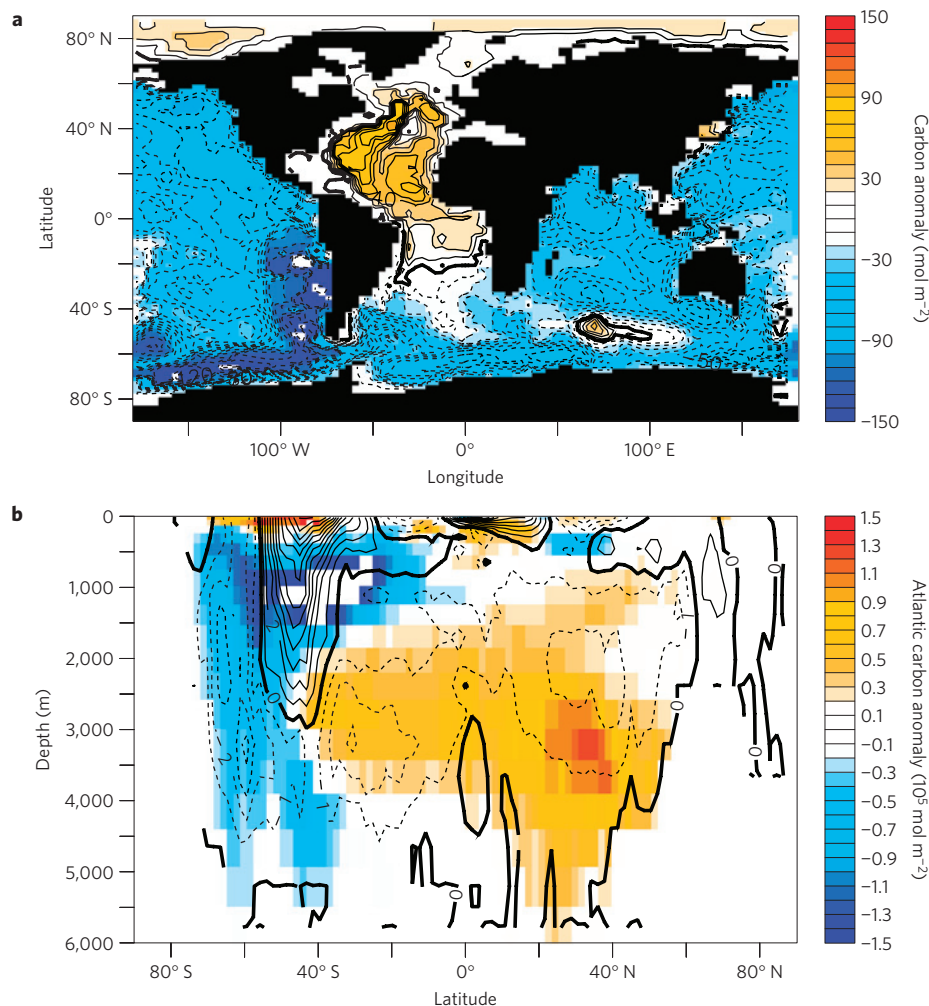


Figure 2 | Equilibrium ocean carbon storage. **a**, Ensemble mean ocean total carbon anomaly (column inventory) of the 18 CMIP3 wind-stress experiments. **b**, Ensemble mean zonally integrated total carbon anomaly for the Atlantic ocean is given by the shading. Contours show the ensemble mean global meridional overturning stream-function anomaly. The contour interval is 1 Sv. All anomalies are computed relative to the control simulation forced with observed pre-industrial winds, and are based on the mean over 6,900–7,000 years.

the separate effects of the pre-industrial equilibrium wind-stress bias and the transient wind-stress impact.

Carbon emissions increased atmospheric CO_2 concentrations, altered the air–sea p_{CO_2} gradient and forced a net oceanic uptake of carbon across all of the CMIP3 transient simulations, and the control simulation forced with observed pre-industrial winds. Natural outgassing of carbon from the ocean (Fig. 4b) was reduced owing to increasing atmospheric CO_2 concentrations, and a decreasing Δp_{CO_2} in the tropical upwelling regions for all of the simulations, and led to the net oceanic uptake. Over periods in which the deep-ocean circulation becomes important, there are significant differences in the rate of ocean carbon uptake amongst the simulations (Fig. 4a). All of the CMIP3 runs uptake more carbon than the control run. In total, by 2200 there is a 100 Pg range in total ocean carbon uptake amongst the CMIP3 runs. This represents an uncertainty amongst the models of roughly 10% of the 1,000 Pg of total ocean carbon uptake since 1850.

The principal reason for the increased ocean carbon storage by the CMIP3 experiments relative to the control is an anomalous reduction in oceanic outgassing of carbon from the principal natural outgassing regions in the tropical Pacific (Fig. 4c). The predominant signal in the tropics is related to the air–sea p_{CO_2} gradient. Here, the intermediate water upwelling in the CMIP3 wind simulations had a lower carbon content than the control

(see Fig. 1a), leading to a reduced p_{CO_2} gradient and a decrease in equatorial outgassing in the CMIP3 wind simulations, relative to the control. Thus, inter-experiment differences in uptake rates during the transient simulations are principally due to differences in the ocean's sub-surface carbon concentration. The pre-industrial wind-stress bias led to a bias in the sub-surface ocean carbon initial condition of the transient experiments, causing these low deep-water carbon concentrations and increased uptake of atmospheric CO_2 . This over-estimation of ocean carbon sequestration in our CMIP3 transient climate simulations leads to a modest under-estimation of atmospheric CO_2 relative to the control (see Supplementary Information S4).

In the original CMIP3 coupled models the wind stress evolves in time, generally exhibiting a poleward shift over the twentieth and twenty-first centuries^{6,19}. It has previously been shown that the CMIP3 ensemble mean twentieth-century poleward wind shift can increase ocean carbon uptake in transient climate change experiments¹⁸. The pre-industrial initial-condition bias that we describe here is independent of, and greater in magnitude than, the previously described changes induced by the transient poleward wind-stress shifts¹⁸. Note that our results pertain to a single climate model, forced by different wind stresses. Caution should be used in generalizing these results to inter-model or model–observation comparisons, because other uncertainties

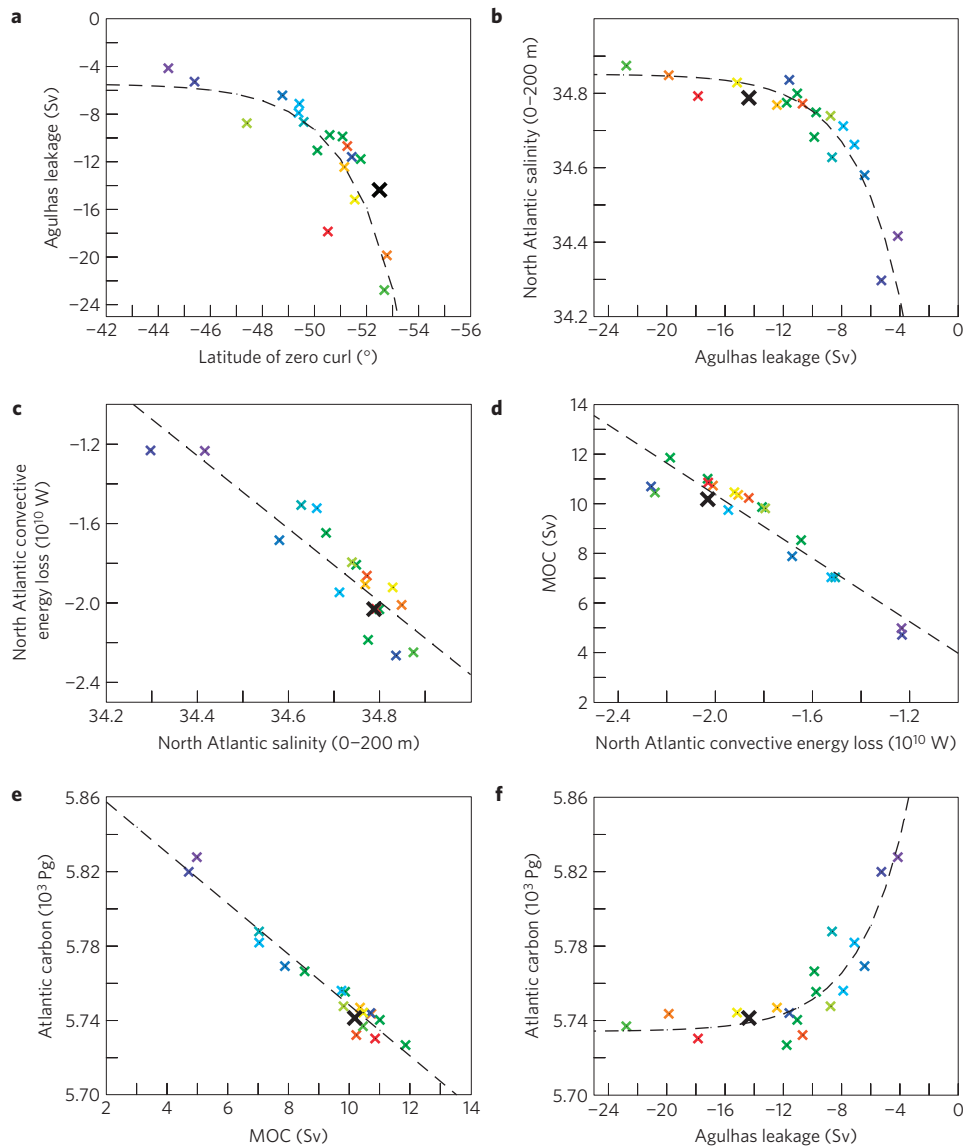


Figure 3 | Equilibrium carbon–circulation relations. **a**, Latitude of zero wind-stress curl over the Indian Ocean (mean 20°–40° E) versus Agulhas leakage at 20° E. **b**, Agulhas leakage (20° E) versus mean North Atlantic salinity in the upper 200 m. **c**, Mean North Atlantic salinity (0–200 m) versus energy loss from convection in the North Atlantic. **d**, Energy loss from convection in the North Atlantic versus global meridional overturning stream function (mean 500–2,000 m, 30° S–60° N). **e**, Mean MOC stream-function (500–2,000 m, 30° S–60° N) versus Atlantic carbon (30° S–60° N). **f**, Atlantic carbon (30° S–60° N) versus Agulhas leakage (20° E). All variables are plotted on the basis of the equilibrium experiment 6,900–7,000-year mean. Dashed lines represent exponential (**a,b,f**) and linear (**c,d,e**) least-squares fits to the data. The colour scheme for the markers corresponds to Fig. 1. The heavy black markers show the control, forced with observed pre-industrial winds.

in ocean carbon uptake may influence the signal that we have described.

We have isolated and quantified one out of several potential uncertainties in modelled ocean carbon uptake rates. Present climate model wind-stress biases will reduce pre-industrial ocean carbon storage, as well as increase ocean carbon uptake and reduce atmospheric CO₂ in transient climate change simulations, relative to simulations with unbiased winds that are otherwise identical. The CMIP3 spread of wind-stress biases led to an uncertainty in ocean carbon uptake of approximately 10% by 2200. Our findings should help with interpreting uncertainties in the next generation of coupled carbon–climate models being used in the CMIP5 exercise.

Methods

To evaluate the bias in the CMIP3 pre-industrial wind stresses, we computed a best estimate of the observed pre-industrial wind stress using four reanalysis products including the new NOAA–CIRES (National Oceanic and Atmospheric

Administration–Cooperative Institute for Research in Environmental Sciences) twentieth-century reanalysis²⁰ (see Supplementary Information S1). The CMIP3 ensemble mean and many of the individual CMIP3 models pre-industrial winds in the Southern Hemisphere are statistically significantly equatorward displaced, and significantly stronger than the observed pre-industrial winds (Supplementary Fig. S1 and Table S1). The biases in the CMIP3 model winds are much larger than the uncertainties in observed winds (Supplementary Table S1). The model biases in wind-stress position (about 3°) are of the same order as the meridional resolution of the model grid (1.8°), yet they are well resolved because their scale is much smaller than that of the westerly wind jet (about 30°; ref. 21).

For our climate simulations we used version 2.9 of the intermediate complexity UVic ESCM (ref. 3). The UVic ESCM has a fully dynamic three-dimensional ocean general circulation model²², including the mixing parametrization of ref. 23, a full explicit scheme for vertical convection²² and the parametrization of subgrid-scale eddy mixing of ref. 24 (see Supplementary Information S3 for a consideration of the physical processes resolved by the model). The ocean model is coupled to a one-layer energy–moisture balance atmosphere model, a thermodynamic–dynamic sea ice model and a simple land surface model, all of which have been fully described previously³. Surface wind stress, surface wind

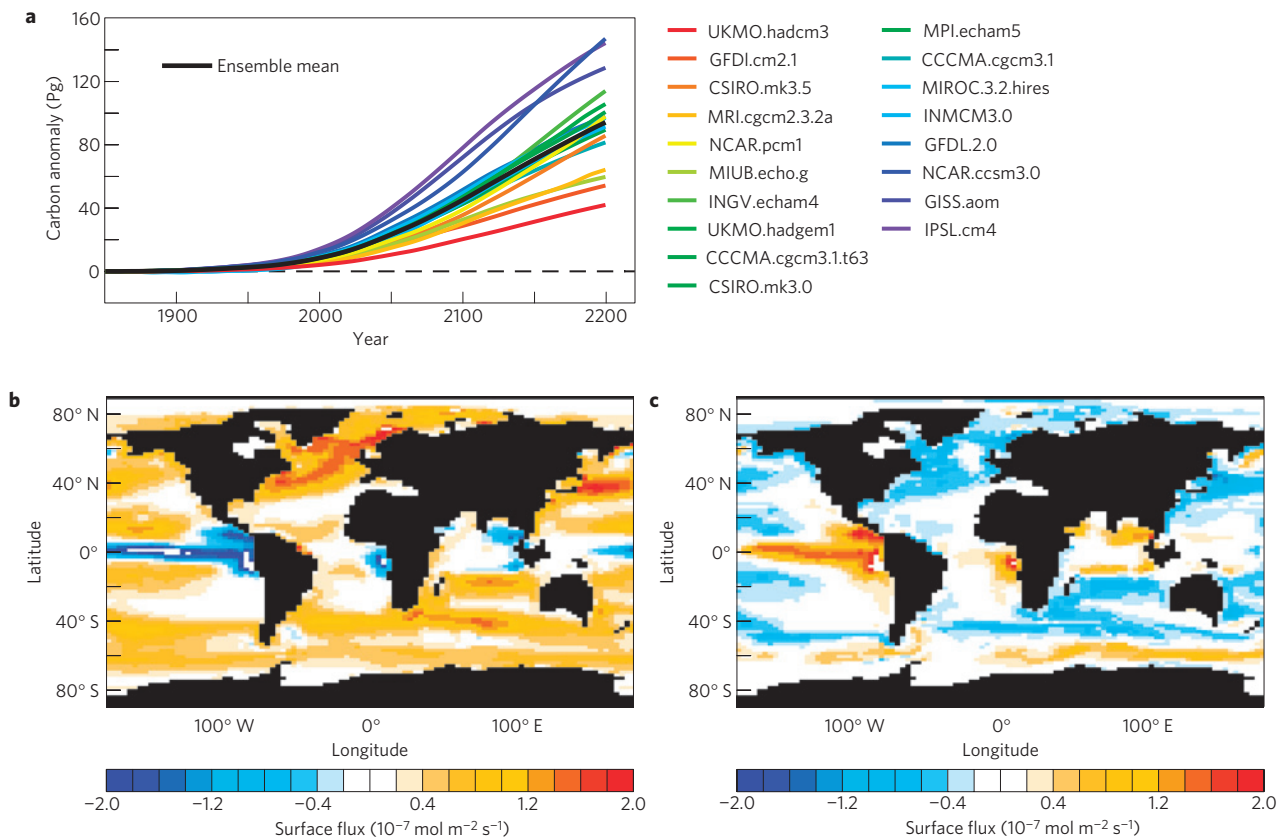


Figure 4 | Transient ocean carbon uptake. **a**, Total ocean carbon uptake anomaly for the 18 CMIP3 experiments, relative to the control simulation with observed winds. The black line shows the ensemble mean uptake anomaly. **b**, Ensemble mean surface CO_2 flux of the 18 CMIP3 experiments at year 2200. **c**, Ensemble mean surface CO_2 flux anomaly. Anomalies are computed as the CMIP3 experiment ensemble mean at year 2200 minus the ensemble mean at 1850, minus the control simulation difference (2200–1850). The transient experiments used the end point of the equilibrium experiments (Fig. 1a) as their initial condition. All forcing, including wind stress, was held constant at pre-industrial levels, except for atmospheric CO_2 emissions, which increased from 1850 to 2100 according to the SRES A2 scenario, and then were held fixed (see text for details).

speed and vertically averaged advective atmospheric winds are specified owing to the simplified nature of the model's atmosphere. The model components share a global domain with a horizontal resolution of 3.6° longitude by 1.8° latitude. Twentieth-century simulations of the UVic ESCM produce realistic distributions of zonal mean temperature and salinity in the ocean, and surface air temperatures in the atmosphere³.

The UVic model incorporates a state-of-the-art carbon cycle, including an oceanic inorganic carbon cycle model³, a marine ecosystem model²⁵ and a land surface and vegetation model²⁶. The UVic ESCM was evaluated as part of the Coupled Carbon Cycle Climate Model Intercomparison Project⁴ and the Paleoclimate Modelling Intercomparison Project²⁷. The characteristics of the coupled climate–carbon cycle system, including the air–sea flux of CO_2 , the distribution of ocean dissolved inorganic carbon and alkalinity, have previously been extensively evaluated for the UVic ESCM, and found to be in good agreement with observations⁸. The evolution of atmospheric CO_2 , surface air temperatures and ocean carbon uptake in previous transient simulations by the UVic ESCM over the twentieth century also generally match observational estimates within uncertainty⁸.

In our study we started the UVic ESCM from an established pre-industrial equilibrium and produced a 7,000-year-long control run under constant 1850 atmospheric CO_2 concentrations (283.9 ppm). The control run was forced with our best estimate of the observed pre-industrial wind stress. For 18 models that submitted wind-stress fields to the World Climate Research Programme's CMIP3 archive⁹, a monthly zonal wind-stress climatology was created using the last 100 years of the pre-industrial control experiment. We then conducted 18 equilibrium experiments, which were also integrated for 7,000 years under constant 1850 atmospheric CO_2 concentrations, using the 18 individual CMIP3 pre-industrial zonal wind-stress climatologies. These experiments are compared with the 7,000-year control run in this work. The only difference between the control run and the experiments was the surface wind-stress field over the ocean.

From the end of the equilibrium runs, we launched transient CO_2 experiments, spanning the period 1850–2200. During the transient runs, CO_2 concentrations were allowed to evolve freely and CO_2 emissions into the atmosphere were

specified on the basis of observations until the year 2000 and then following the SRES A2 scenario (A2 from 2000 to 2100; after 2100 emissions are held constant). All other forcings were held at 1850 levels during the transient runs. In the transient experiments, we continued to force the 18-member ensemble with the CMIP3 pre-industrial winds, and the control simulation forcing remained the best estimate of the observed pre-industrial wind stress. The wind stress was held fixed to isolate the effect of the pre-industrial wind-stress bias on the transient simulations.

Received 20 April 2011; accepted 12 October 2011; published online 13 November 2011

References

- Russell, J., Stouffer, R. J. & Dixon, K. Intercomparison of the Southern Ocean circulations in IPCC coupled model control simulations. *J. Clim.* **19**, 4560–4575 (2006).
- Sijp, W. & England, M. The effect of a northward shift in the Southern Hemisphere westerlies on the global ocean. *Prog. Oceanogr.* **79**, 1–19 (2008).
- Weaver, A. *et al.* The UVic Earth System Climate Model: Model description, climatology, and applications to past, present and future climates. *Atmos. Ocean* **39**, 1–68 (2001).
- Friedlingstein, P. *et al.* Climate–carbon cycle feedback analysis: Results from the C4MIP model intercomparison. *J. Clim.* **19**, 3337–3353 (2006).
- Meredith, M., Naveira Garabato, A., Hogg, A. M. & Farneti, R. Sensitivity of the overturning circulation in the Southern Ocean to decadal changes in wind forcing. *J. Clim.* (in the press).
- Fyfe, J. & Saenko, O. Simulated changes in the extratropical Southern Hemisphere winds and currents. *Geophys. Res. Lett.* **33**, L06701 (2006).
- Russell, J., Dixon, K., Gnanadesikan, A., Stouffer, R. & Toggweiler, J. The Southern Hemisphere Westerlies in a warming world: Propping open the door to the deep ocean. *J. Clim.* **19**, 6382–6390 (2006).

8. Eby, M. *et al.* Lifetime of anthropogenic climate change: Millennial time scales of potential CO₂ and surface temperature perturbations. *J. Clim.* **22**, 2501–2511 (2009).
9. Meehl, G. A. *et al.* The WCRP CMIP3 multi-model dataset: A new era in climate change research. *Bull. Am. Meteorol. Soc.* **88**, 1383–1394 (2007).
10. Hibbard, K., Meehl, G. A., Cox, P. M. & Friedlingstein, P. A strategy for climate change stabilization experiments. *Eos* **88**, 217–221 (2007).
11. Beal, L. *et al.* On the role of the Agulhas system in ocean circulation and climate. *Nature* **472**, 429–436 (2011).
12. Peeters, F. *et al.* Vigorous exchange between the Indian and Atlantic oceans at the end of the past five glacial periods. *Nature* **430**, 661–665 (2004).
13. Biastoch, A., Boning, C. W., Schwarzkopf, F. U. & Lutjeharms, J. R. E. Increase in Agulhas leakage due to poleward shift of Southern Hemisphere westerlies. *Nature* **462**, 495–498 (2009).
14. Weijer, W., de Ruijter, W., Dijkstra, H. & van Leeuwen, P. Impact of interbasin exchange on the Atlantic overturning circulation. *J. Phys. Oceanogr.* **29**, 2266–2284 (1999).
15. Biastoch, A., Boning, C. W. & Lutjeharms, J. R. E. Agulhas leakage dynamics affects decadal variability in Atlantic overturning circulation. *Nature* **456**, 489–492 (2008).
16. Sijp, W. & England, M. Southern Hemisphere westerly wind control over the ocean's thermohaline circulation. *J. Clim.* **22**, 1277–1286 (2009).
17. Meehl, G. A. *et al.* in *IPCC Climate Change 2007: The Physical Science Basis* (eds Solomon, S. *et al.*) 747–845 (Cambridge Univ. Press, 2007).
18. Zickfeld, K., Fyfe, J., Saenko, O., Eby, M. & Weaver, A. Response of the global carbon cycle to human-induced changes in Southern Hemisphere winds. *Geophys. Res. Lett.* **34**, L12712 (2007).
19. Kidston, J. & Gerber, E. Intermodel variability of the poleward shift of the austral jet stream in the CMIP3 integrations linked to biases in 20th century climatology. *Geophys. Res. Lett.* **37**, L09708 (2010).
20. Compo, G. P. *et al.* The twentieth century reanalysis project. *Q. J. R. Meteorol. Soc.* **137**, 1–28 (2011).
21. Kushner, P., Held, I. & Delworth, T. Southern Hemisphere atmospheric circulation response to global warming. *J. Clim.* **14**, 2238–2249 (2001).
22. Pacanowski, R. *Mom 2 Documentation, User's Guide and Reference Manual* GFDL Ocean group Tech. Rep. 3 (NOAA/GFDL, 1995).
23. Bryan, K. & Lewis, L. A water mass model of the world ocean. *J. Geophys. Res.* **84**, 2503–2517 (1979).
24. Gent, P. & McWilliams, J. Isopycnal mixing in ocean circulation models. *J. Phys. Oceanogr.* **20**, 150–155 (1990).
25. Schmittner, A., Oeschies, A., Giraud, X., Eby, M. & Simmons, H. L. A global model of the marine ecosystem for long-term simulations: Sensitivity to ocean mixing, buoyancy forcing, particle sinking, and dissolved organic matter cycling. *Glob. Biogeochem. Cycles* **19**, GB3004 (2005).
26. Meissner, K. J., Weaver, A. J., Matthews, H. D. & Cox, P. M. The role of land surface dynamics in glacial inception: A study with the UVic Earth System Model. *Clim. Dyn.* **21**, 515–537 (2003).
27. Weber, S. L. *et al.* The modern and glacial overturning circulation in the Atlantic ocean in PMIP coupled model simulations. *Clim. Past* **3**, 51–64 (2007).

Acknowledgements

N.C.S. received financial support from the National Research Foundation of South Africa, and through the NSERC CREATE training programme in interdisciplinary climate science at the University of Victoria, Canada. We thank the UVic Climate Modelling Group, in particular M. Eby, A. Weaver and E. Wiebe, for help with the UVic ESCM. This research has been enabled by the use of computing resources provided by WestGrid and Compute/Calcul Canada. We acknowledge the modelling groups, the Program for Climate Model Diagnosis and Intercomparison and the WCRP's Working Group on Coupled Modelling for their roles in making available the WCRP CMIP3 multi-model data set. Support of this data set is provided by the Office of Science, US Department of Energy. J. Christian, M. Eby, N. Gillet and J. Scinocca provided useful comments on an early draft of the manuscript.

Author contributions

J.C.F. conceived of the experiment, advised on the analysis, helped to interpret the results and edited the paper. N.C.S. designed the experiment, conducted the model runs, analysed the output, interpreted the results and wrote most of the paper.

Additional information

The authors declare no competing financial interests. Supplementary information accompanies this paper on www.nature.com/natureclimatechange. Reprints and permissions information is available online at <http://www.nature.com/reprints>. Correspondence and requests for materials should be addressed to N.C.S.